

# We are IntechOpen, the world's leading publisher of Open Access books Built by scientists, for scientists

6,900

Open access books available

186,000

International authors and editors

200M

Downloads

Our authors are among the

154

Countries delivered to

TOP 1%

most cited scientists

12.2%

Contributors from top 500 universities



WEB OF SCIENCE™

Selection of our books indexed in the Book Citation Index  
in Web of Science™ Core Collection (BKCI)

Interested in publishing with us?  
Contact [book.department@intechopen.com](mailto:book.department@intechopen.com)

Numbers displayed above are based on latest data collected.  
For more information visit [www.intechopen.com](http://www.intechopen.com)



# Atom Substitution Effects in Ionic Liquids: A Microscopic View by Femtosecond Raman- Induced Kerr Effect Spectroscopy

Hideaki Shirota and Hiroki Fukazawa

*Department of Nanomaterial Science & Department of Chemistry*

*Chiba University*

*Japan*

## 1. Introduction

It is well known that the physical and chemical properties of ionic liquids (ILs) vary when the combination of cations and anions changes. It is thus possible to tune the properties of ILs on demand by choosing a suitable cation and anion combination. Consequently, ILs are commonly referred to as designer fluids. Many studies have demonstrated the usefulness of this strategy for controlling the properties of ILs (Wasserscheid & Welton, 2008; Ohno, 2005). It is possible to systematically examine the physical and chemical properties of ILs by changing an ionic species, while leaving a counter ion unchanged, in order to understand the relationships between an IL's chemical and physical properties and its constituent ion species. Extensive efforts along this line of study have clarified the relationships between the physical and chemical properties and the ionic species.

On the other hand, the effects of replacing an atomic element in an ionic species on the physical and chemical properties of ILs have not been very well understood. It is obvious that one of the main themes in chemistry is to develop an understanding of how chemical and physical properties depend on the atomic elements in molecular liquids as well as in ILs. In 2005, C and Si in a side group of an imidazolium cation (1-methyl-3-neopentylimidazolium: [C-MIm]<sup>+</sup> and 1-methyl-3-trimethylsilylmethylimidazolium: [Si-MIm]<sup>+</sup>) were compared (Shirota & Castner, 2005). The shear viscosities of the silicon substituted ILs are substantially reduced in comparison with those of the respective carbon ILs, when ILs with the same anions are compared. Actually, this feature of ILs is the opposite of that observed in conventional neutral molecular liquids. For example, the shear viscosity of bromobenzene at a standard ambient condition is approximately 1.4 times larger than that of chlorobenzene, and the ambient shear viscosity of diethyl sulfide is approximately 1.9 times larger than that of diethyl ether (Lide, 2008). Heavier atom substitution in the hexafluoropnictogenate anion ([XF<sub>6</sub>]<sup>-</sup>; X: P, As, and Sb) for 1-butyl-3-methylimidazolium ILs also gives a lower shear viscosity (Shirota et al., 2009). In addition to aromatic cation-based ILs, reductions in the shear viscosities of ILs with heavier atoms in the same position were also confirmed in nonaromatic cation-based ILs (Tsunashima & Sugiya, 2007; Seki et al., 2009; Shirota et al., 2010).

Interionic interaction is a key parameter for determining the physical and chemical properties of ILs. Because the interionic interactions in ILs are delicately balanced between

the attractive and repulsive forces, the salts fit to be a liquid at room temperature. The physical properties of ILs depend on the interionic interaction. Therefore, it is important to gain an in-depth understanding of the molecular-level aspects of the interionic interaction in ILs. Intermolecular vibration in condensed phases is a measure of the microscopic intermolecular interaction. Most intermolecular vibrations in condensed phases are in the frequency range of approximately 1–150  $\text{cm}^{-1}$ . Several groups have studied the interionic vibrations in this low frequency region to reveal the microscopic structure and interaction in ILs using sophisticated time-resolved spectroscopic techniques such as femtosecond Raman-induced Kerr effect spectroscopy (RIKES) (Castner et al., 2007) and terahertz time-domain spectroscopy (THz-TDS) (Asaki et al., 2002; Yamamoto et al., 2007; Koeberga et al., 2007) as well as steady-state low-frequency Raman and far-infrared spectroscopies (Dominguez-Vidal et al., 2007; Iwata et al., 2007; Fumino et al., 2008; Buffeteau et al., 2010). Among these spectroscopic techniques, femtosecond RIKES can cover the frequency range of the intermolecular (interionic) vibrational band in molecular liquids including ILs.

Quitevis and co-workers reported the first RIKES-based study of ILs in 2002 (Hyun et al., 2002). The Quitevis group extensively studied the detailed aspects for the microstructures of neat ILs (Xiao et al., 2009; Russina et al., 2010), as well as binary IL mixtures (Xiao et al., 2006; Xiao et al., 2007; Xiao et al., 2008). They also reported a temperature dependent experiment (Rajian et al., 2004). Wynne and co-workers examined the interionic vibrational dynamics in some imidazolium cation-based ILs with different cation and anion combinations and found that an anion substitution produced a significant difference in the interionic vibrations of the ILs (Giraud et al., 2003). A similar feature was also observed in nonaromatic cation-based ILs (Shirota et al., 2005). Wynne's group also compared the low-frequency Kerr spectra of a few ILs with the spectra measured by THz-TDS and dielectric spectroscopy (Turton et al., 2009). We demonstrated some comparative studies such as IL vs. neutral binary solution (Shirota & Castner) and ILs vs. concentrated electrolyte solutions (Fujisawa et al., 2009) using femtosecond RIKES to bring out the unique natures of the ILs. Several novel silyl- and siloxy-group-substituted imidazolium-based ILs were also compared (Shirota et al., 2007). Fayer and co-workers focused on the slower dynamical processes, which included  $\alpha$ - and  $\beta$ -relaxations and the crossover process between intermolecular vibrations and  $\alpha$ -relaxation, and examined the adequacy of the mode coupling theory for several imidazolium-based ILs (Cang, 2003; Li, 2006). Some theoretical studies based on molecular dynamics (MD) simulations further explored deeper molecular aspects of the intermolecular dynamics of ILs reported in the experimental studies. Urahata and Ribeiro performed MD simulations for some imidazolium-based ILs and compared their results with the experimental data reported by Wynne and co-workers (Urahata & Ribeiro, 2005). Their study showed that the density of states profile for the cation was similar to the experimental Kerr spectrum shape. Hu et al. also computed the Kerr spectrum of 1-methoxyethylpyridinium dicyanamide and compared it with the experimental Kerr spectrum (Hu et al., 2008). They showed the importance of the interaction-induced motion on nanosecond timescale, which is not dominant for neutral molecular liquids. Although these studies reveal detailed molecular aspects of the ultrafast dynamics in ILs and help to provide a better and deeper understanding of ILs, we will focus on the heavy atom substitution effects in ILs rather than the studies in this chapter. We will provide an overview of the heavy atom substitution effects in ILs on some static physical properties and will discuss the features using the microscopic interionic interaction investigated by measuring the interionic vibrations with femtosecond RIKES.

## 2. Femtosecond Raman-induced Kerr effect spectroscopy: principle and data analysis

Femtosecond RIKES is a third-order nonlinear spectroscopic technique (McMorrow et al., 1988; Lotshaw et al., 1995; Righini, 1993). This spectroscopic technique can be used to observe the molecular motions such as the reorientation and inter- and intramolecular vibrations in time domain within a range of approximately  $10^{-14}$  to  $10^{-9}$  s. Fig. 1 shows a schematic diagram of the basic principle of femtosecond RIKES. The first (pump) pulse produces a vibrational coherence between  $\omega_1$  and  $\omega_2$  (impulsive Raman process). Then, the second (probe) pulse, which arrives at time  $\tau$  from the first pulse, induces the Raman scattering,  $\omega_s$ . It should be noted that a femtosecond laser pulse is sufficiently short in time domain to obtain a wide spectrum in frequency domain, which shows the intermolecular vibrations and some intramolecular vibrational modes with the frequencies smaller than  $\omega_1 - \omega_2$  ( $\leq \nu_n$ ). Typical femtosecond RIKES can be used to detect the signal by mixing it with a local oscillator. This method is referred to as the optical heterodyne detection and is used to enhance the signal and obtain a linear response to the signal polarization/electric field (Mukamel, 1995). This pump-probe spectroscopic technique is also referred to as optical Kerr effect (OKE) spectroscopy. The difference between the two spectroscopic techniques is attributed to the number of light sources (different colors) used. However, if the light source is a spectrally broad pulse such as a femtosecond pulse, the two spectroscopic techniques are interchangeable. We use the acronym RIKES for the spectroscopic technique in this chapter.

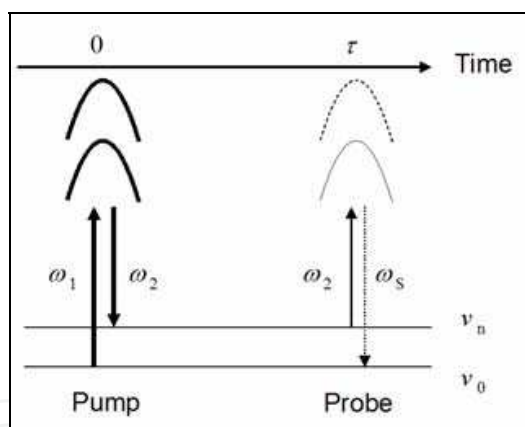


Fig. 1. Schematic diagram of Raman-induced Kerr effect signal.

Femtosecond RIKES can provide a high-quality low-frequency spectrum with the frequency range of approximately  $0.2$ – $750$   $\text{cm}^{-1}$  via Fourier-transform deconvolution analysis (McMorrow & Lotshaw, 1990; McMorrow & Lotshaw, 1991). As an example, Fig. 2 shows the Kerr transient and the Fourier-transform Kerr spectra of ethylbenzene. The femtosecond RIKES directly captures a Kerr transient in time domain, as shown in Fig. 2a. In time-domain data, the diffusive orientational relaxation with a timescale greater than a few picoseconds is often characterized by a multi-exponential function (a biexponential function in the case of ethylbenzene, as shown in Fig. 2a). The Kerr transient is then analyzed by carrying out a Fourier-transform deconvolution procedure using the instrument's response, which is characterized by the cross correlation of the pump and probe pulses in a RIKES system. A Fourier-transform Kerr spectrum with the frequency range of  $0$ – $750$   $\text{cm}^{-1}$  is shown

in Fig. 2b. Clear intramolecular vibrational modes are observed at 156, 486, 556, and 621  $\text{cm}^{-1}$ . The broad band located in below 150  $\text{cm}^{-1}$  is caused by the intermolecular vibrations. In order to discuss the intermolecular vibrational band, the contribution of the diffusive orientational relaxation ( $\tau_2$ ) is subtracted from the entire Kerr spectrum. An enlarged view of the low frequency region is shown in Fig. 2c. It should be noted that the depolarization condition is used for the RIKES setups discussed here (the polarization angles are  $0^\circ$  for the pump,  $+45^\circ$  for the probe, and  $-45^\circ$  for the analyzer). Accordingly, the diffusive orientational relaxation for a spherical molecule is forbidden, and the isotropic vibrational modes are silent for this spectroscopic condition. It is also possible to detect the isotropic vibrational modes by changing the polarization angles for the spectroscopic setup (Khalil et al., 2000; Wiewior et al., 2002; Heisler & Meech, 2010).

Line-shape analysis is also carried out to characterize the Kerr spectra. A common model used to fit a low-frequency Kerr spectrum is the sum of the Bucaro-Litovitz ( $I_{\text{BL}}(\omega)$ ) (Bucaro & Litovitz, 1971) and antisymmetrized Gaussian functions ( $I_{\text{G}}(\omega)$ ) (Chang & Castner, 1993).

$$I_{\text{BL}}(\omega) = A_{\text{BL}} \omega^\alpha \exp(-\omega / \omega_{\text{BL}}) \quad (1)$$

$$I_{\text{G}}(\omega) = A_{\text{G}} \{ \exp[-2(\omega - \omega_{\text{G}})^2 / \Delta\omega_{\text{G}}^2] - \exp[-2(\omega + \omega_{\text{G}})^2 / \Delta\omega_{\text{G}}^2] \} \quad (2)$$

where  $A_n$  is the amplitude parameter,  $\omega_n$  is the characteristic frequency parameter, and  $\Delta\omega_n$  is the width parameter for the model functions. When the index  $\alpha$  in Eq. 1 is unity, the function is an Ohmic function. We used an Ohmic function rather than a Bucaro-Litovitz function to fit the Kerr spectra for simplicity. The Bucaro-Litovitz function was developed to express the depolarized light scattering in atomic and molecular liquids (Bucaro & Litovitz, 1971). The antisymmetrized Gaussian function is assumed to be an inhomogeneously broadened vibrational mode (often regarded as a librational mode) and has been empirically used to fit the low-frequency Kerr spectrum in molecular liquids (Chang & Castner, 1993). In reality, the model functions do not express the shape of a motion in spectrum, but this analysis is useful to qualitatively discuss the spectral feature. Although the multi-mode Brownian oscillator model (Tanimura & Mukamel, 1993; Nagata & Tanimura, 2006) is also commonly used to characterize the low-frequency spectra (Giraud et al., 2003; Shirota et al., 2005), the former analytical model is used throughout this chapter.

Most of the earlier femtosecond RIKES studies were conducted to clarify the intermolecular vibrational and orientational dynamics in pure molecular liquids and binary mixtures (Kinoshita et al., 1996; Castner & Maroncelli, 1998; Smith & Meech, 2002; Zhong & Fourkas, 2008; Shirota et al., 2009). Nowadays, femtosecond RIKES is also used to study the intermolecular vibrational dynamics, reorientation, and microscopic intermolecular interactions of complex condensed phases (Hunt et al., 2007; Farrer & Fourkas, 2003) such as polymer liquids and solutions, microemulsions, aqueous protein films and solutions, and solvents in nanoporous glasses. As mentioned above, femtosecond RIKES has also been used to investigate ILs (Castner et al., 2007).

The details of the femtosecond RIKES setups used for the studies described in this chapter have been reported elsewhere (Wiewior et al., 2002; Shirota, 2005; Shirota et al., 2009). In short, the light sources for the setups were titanium:sapphire lasers pumped by approximately 3.5 W of 532-nm light from a neodymium:vanadate laser (Spectra Physics). The center wavelength of the titanium:sapphire lasers was 800–810 nm, with a full width at half maximum value of ca. 60 or 75 nm and a repetition frequency of ca. 85 MHz. The output

power was 300–350 mW. The temporal response for the femtosecond RIKES setups was approximately 30–40 fs.

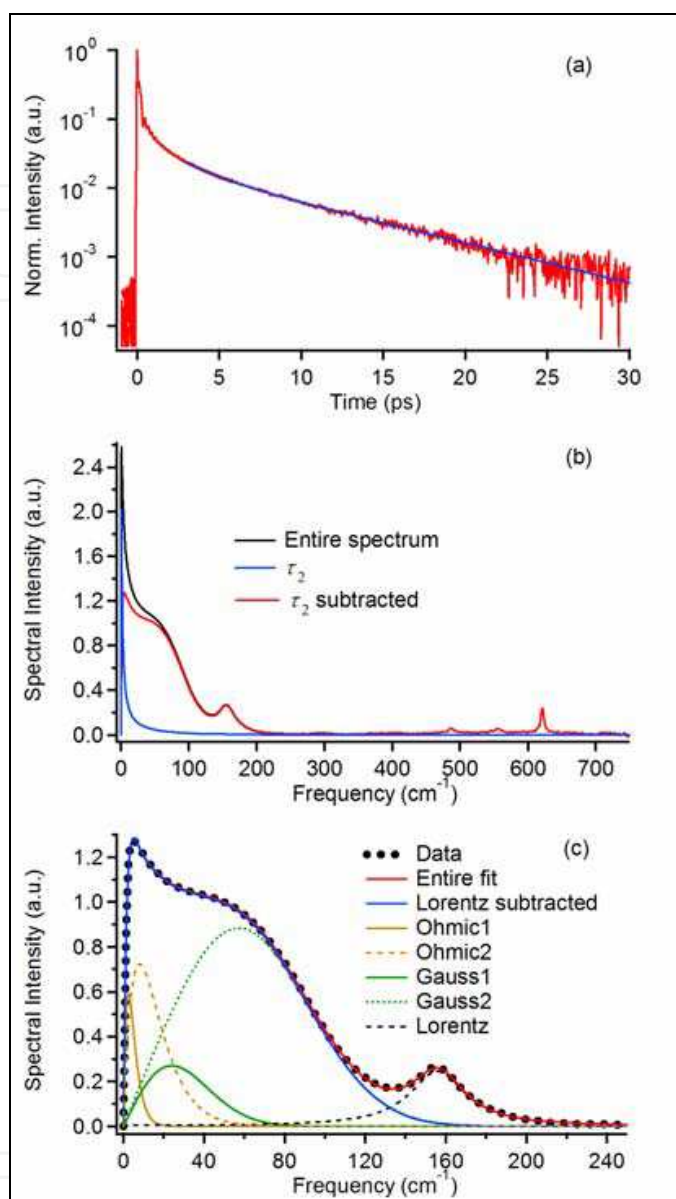


Fig. 2. (a) Kerr transient of liquid ethylbenzene (red) and its biexponential fit (blue). The fit starts from 3 ps. (b) Fourier-transform Kerr spectrum (black), contribution of the slowest relaxation time  $\tau_2$  (blue), and  $\tau_2$ -subtracted Kerr spectrum (red). (c) Magnification of the  $\tau_2$ -subtracted Kerr spectrum. The black dotted line, red line, brown lines, green lines, black broken line, and blue line denote the Fourier-transform Kerr spectrum, its entire fit, Ohmic functions, antisymmetrized Gaussian functions, Lorentzian function, and Lorentzian function subtracted spectrum, respectively.

### 3. Target ionic liquids, electronic structures, and static properties

The sample ILs discussed in this chapter were synthesized according to the standard procedure (Wasserscheid & Welton, 2008; Saurez et al., 1998; Holbrey & Seddon, 1999;

Dzyuba & Bartsch, 2002; Tsunashima & Sugiya, 2007), except for 1-butyl-3-methylimidazolium hexafluorophosphate ([BMIm][PF<sub>6</sub>], Wako Pure Chemical) and 1-butyl-3-methylimidazolium hexafluoroantimonate ([BMIm][SbF<sub>6</sub>], Fluka), which were used as received. Before the measurements, the ILs were dried in vacuo, typically at approximately 315 K for 36 h. The details of these sample ILs have been described elsewhere (Shirota & Castner, 2005; Shirota et al., 2009; Shirota et al., 2010). The ILs and their abbreviations are as follows.

1-Methyl-3-neopentylimidazolium bis(trifluoromethylsulfonyl)amide: [C-MIm][NTf<sub>2</sub>]; 1-methyl-3-trimethylsilylmethylimidazolium bis(trifluoromethylsulfonyl)amide: [Si-MIm][NTf<sub>2</sub>]; 1-methyl-3-neopentylimidazolium tetrafluoroborate: [C-MIm][BF<sub>4</sub>]; 1-methyl-3-trimethylsilylmethylimidazolium tetrafluoroborate: [Si-MIm][BF<sub>4</sub>]; 1-butyl-3-methylimidazolium hexafluoroarsenate: [BMIm][AsF<sub>6</sub>]; triethyloctylammonium bis(trifluoromethylsulfonyl)amide: [N<sub>2228</sub>][NTf<sub>2</sub>]; triethyloctylphosphonium bis(trifluoromethylsulfonyl)amide: [P<sub>2228</sub>][NTf<sub>2</sub>]; (2-ethoxyethoxy)ethyltriethylammonium bis(trifluoromethylsulfonyl)amide: [N<sub>222(2O2O2)</sub>][NTf<sub>2</sub>]; (2-ethoxyethoxy)ethyltriethylphosphonium bis(trifluoromethylsulfonyl)amide: [P<sub>222(2O2O2)</sub>][NTf<sub>2</sub>]; (2-ethoxyethoxy)ethyltriethylammonium hexafluorophosphate: [N<sub>222(2O2O2)</sub>][PF<sub>6</sub>]; (2-ethoxyethoxy)ethyltriethylphosphonium hexafluorophosphate: [P<sub>222(2O2O2)</sub>][PF<sub>6</sub>]; (2-ethoxyethoxy)ethyltriethylammonium hexafluoroarsenate: [N<sub>222(2O2O2)</sub>][AsF<sub>6</sub>]; (2-ethoxyethoxy)ethyltriethylphosphonium hexafluoroarsenate: [P<sub>222(2O2O2)</sub>][AsF<sub>6</sub>]. The chemical structures of the target cations and anions for the heavy atom substitution studies are shown in Fig. 3.

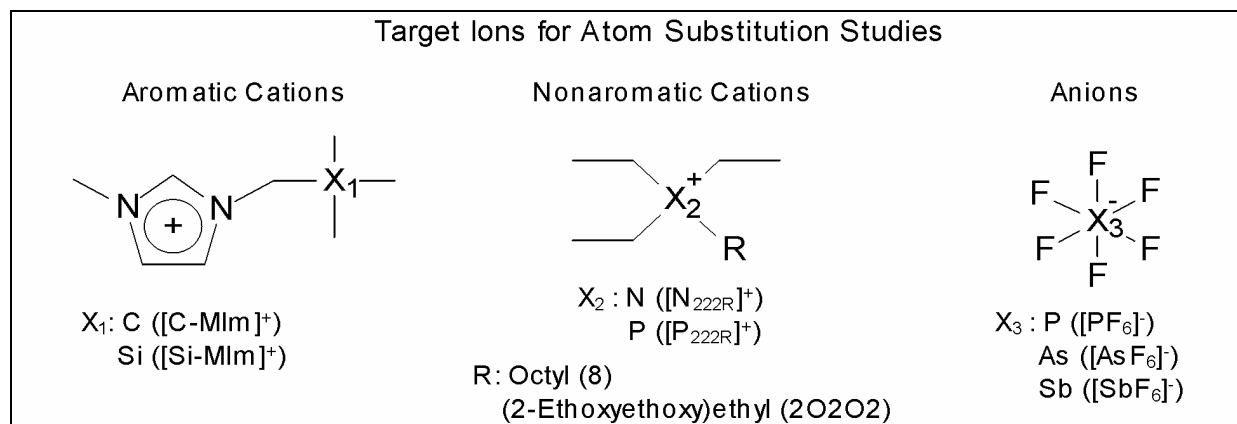


Fig. 3. Chemical structures of target ions for atom substitution studies.

Because ions have charges in nature, it is important to understand the charge magnitudes of the atoms in the ions. Fig. 4 shows the optimized geometries and atom charges of the target ions. The geometry optimization calculations were performed based on the density functional theory of the B3LYP/6-311++G(d,p) level for the [X-MIm]<sup>+</sup> and [X<sub>2228</sub>]<sup>+</sup> cations and the B3LYP/aug-cc-pVDZ or aug-cc-pVDZ-PP level for the [XF<sub>6</sub>]<sup>-</sup> anions. The charges were estimated using the CHelpG algorithm.

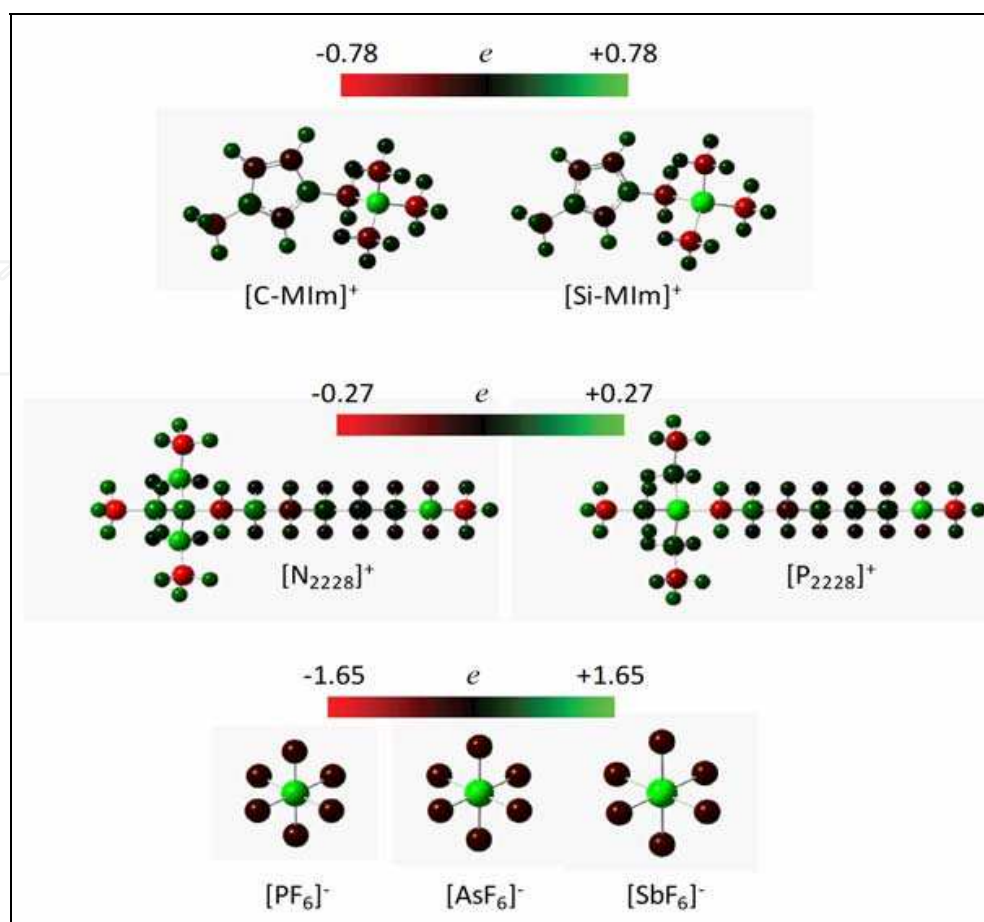


Fig. 4. Atom charges of target ions for atom substitution studies.

Overall, the features of the heavy atom substitutions in the three categories ( $[X\text{-MIm}]^+$ ,  $[X_{2228}]^+$ , and  $[XF_6]^-$ ) were similar. That is, the charge magnitude of the heavier atom in the ions was larger than that of the corresponding lighter atom of the respective ions in most cases: Si in  $[\text{Si-MIm}]^+$  (+0.773) vs. C in  $[\text{C-MIm}]^+$  (+0.602); P in  $[\text{P}_{2228}]^+$  (+0.250) vs. N in  $[\text{N}_{2228}]^+$  (+0.102); Sb in  $[\text{SbF}_6]^-$  (+1.650) vs. As in  $[\text{AsF}_6]^-$  (+1.393) vs. P in  $[\text{PF}_6]^-$  (+1.414). In addition, the bond length of the target atoms became longer with the heavy atom substitution: Si-CH<sub>3</sub> in  $[\text{Si-MIm}]^+$  (1.880 Å) vs. C-CH<sub>3</sub> in  $[\text{C-MIm}]^+$  (1.539 Å); P-CH<sub>2</sub>CH<sub>3</sub> in  $[\text{P}_{2228}]^+$  (1.832 Å) vs. N-CH<sub>2</sub>CH<sub>3</sub> in  $[\text{N}_{2228}]^+$  (1.531 Å); Sb-F in  $[\text{SbF}_6]^-$  (1.937 Å) vs. As-F in  $[\text{AsF}_6]^-$  (1.775 Å) vs. P-F in  $[\text{PF}_6]^-$  (1.660 Å). The ab initio quantum chemistry calculation results thus suggest that the heavy atom substitution in ions produces two opposing features in relation to the interionic interaction. A bigger charge magnitude in an atom produces a stronger interionic interaction at the local site (attractive Coulomb or dipole-dipole interaction), but a larger ionic volume brings a weaker interionic interaction (steric repulsive force).

Table 1 summarizes the data for the liquid density, shear viscosity, and surface tension at 297 K for the sample ILs, as well as their formula weights and molar volumes. The molar volumes were estimated from the formula weights and liquid densities at 297 K. In the data for the liquid densities, the result of the heavy atom substitutions is slightly confusing: C →

Si and N  $\rightarrow$  P in the cations ( $[\text{C-MIm}]^+ \rightarrow [\text{Si-MIm}]^+$  and  $[\text{N}_{222\text{R}}]^+ \rightarrow [\text{P}_{222\text{R}}]^+$ ) decrease the liquid density, whereas P  $\rightarrow$  As  $\rightarrow$  Sb in the anions ( $[\text{PF}_6]^- \rightarrow [\text{AsF}_6]^- \rightarrow [\text{SbF}_6]^-$ ) increase the liquid density. A larger atom definitely has a heavier mass and a larger volume. These effects on the liquid density arising from the heavy atom substitution are thus counterintuitive. If we look at the periodic table, the gap in the atomic masses between the periods 2 and 3 is much smaller than that between the periods 3 and 4 and between the periods 4 and 5 (Lide, 2008). Conversely, the difference in the atomic volumes between the periods 2 and 3 is larger than that between the periods 3 and 4 and between the periods 4 and 5 (Bondi, 1964). As a result, the heavy atom substitutions, C  $\rightarrow$  Si and N  $\rightarrow$  P, in the cations give a lower liquid density as a dominant factor for the volume effect, whereas the heavy atom substitutions, P  $\rightarrow$  As  $\rightarrow$  Sb, in the anions give a higher liquid density as the dominant parameter of the mass effect.

ILs	FW	$d$ (g/mL)	$\eta$ (cP)	$\gamma$ (mN/m)	$V$ (mL/mol)
$[\text{C-MIm}][\text{NTf}_2]$	433.4	1.413	161.4	31.6	306.7
$[\text{Si-MIm}][\text{NTf}_2]$	449.5	1.398	90.7	30.1	321.5
$[\text{C-MIm}][\text{BF}_4]$	240.1	1.207	3337	40.0	198.9
$[\text{Si-MIm}][\text{BF}_4]$	256.1	1.188	546.2	36.8	215.6
$[\text{BMIm}][\text{PF}_6]^a$	248.2	1.368	289.6	43.7	181.4
$[\text{BMIm}][\text{AsF}_6]^a$	328.1	1.540	228.0	44.8	213.1
$[\text{BMIm}][\text{SbF}_6]^a$	375.0	1.690	133.7	45.2	221.9
$[\text{N}_{222}][\text{NTf}_2]^b$	494.6	1.249	227.0	32.8	396.0
$[\text{P}_{222}][\text{NTf}_2]^b$	511.5	1.244	123.3	32.7	411.2
$[\text{N}_{222(2\text{O}_2\text{O}_2)}][\text{NTf}_2]^b$	498.5	1.328	70.4	35.3	375.4
$[\text{P}_{222(2\text{O}_2\text{O}_2)}][\text{NTf}_2]^b$	515.5	1.319	43.7	35.0	390.8
$[\text{N}_{222(2\text{O}_2\text{O}_2)}][\text{PF}_6]^b$	363.3	1.255	699.0	45.0	289.5
$[\text{P}_{222(2\text{O}_2\text{O}_2)}][\text{PF}_6]^b$	380.3	1.250	232.8	44.3	304.2
$[\text{N}_{222(2\text{O}_2\text{O}_2)}][\text{AsF}_6]^b$	407.3	1.381	607.4	45.3	294.9
$[\text{P}_{222(2\text{O}_2\text{O}_2)}][\text{AsF}_6]^b$	424.2	1.368	216.1	44.5	310.1

Table 1. Formula weights FW, liquid densities  $d$ , shear viscosities  $\eta$ , surface tensions  $\gamma$ , and molar volume  $V$  at 297 K for ILs. The data are from <sup>a</sup>Shirota et al., 2009, and <sup>b</sup>Shirota et al., 2010. Data at 297 K for the upper four ILs are newly published data.

In the data for the shear viscosity, the heavy atom substitution effect is clearly observed with the same trend for any ILs: the heavier atom substitution gives a lower shear viscosity. As mentioned previously, this effect is the opposite of that for common neutral molecular liquids (e.g.,  $\eta(\text{fluorobenzene}): 0.550 \text{ cP} < \eta(\text{chlorobenzene}): 0.753 \text{ cP} < \eta(\text{bromobenzene}): 1.074 \text{ cP}$  and  $\eta(\text{diethyl ether}): 0.224 \text{ cP} < \eta(\text{diethyl sulfide}): 0.442 \text{ cP}$  at 298 K (Lide, 2008)). In

general, this effect in conventional molecular liquids arises from the heavier mass and larger molar volume (dispersion force).

In ILs, the ion volume is critical for the interionic interaction strength because the distance between a cation and an anion affects the interionic interaction strength. In the simplest case, e.g., in a spherical ion pair, the Coulombic energy,  $E_{\text{Coulomb}}(r)$ , is inversely proportional to the distance between a cation and an anion:  $E_{\text{Coulomb}}(r) \propto 1/r$  (Israelacvili, 1992). Moreover, the total interaction energy in ionic crystals is proportional to the inverse of the distance between a cation and anion (the Madelung constant) (Israelacvili, 1992). As seen in Table 1, we can confirm that the molar volume in the ILs becomes larger as the cation and anion become heavier. Although the self-diffusion, interionic interaction, and ion-pair formation do not always correlate to the ionic volume (Tsuzuki et al., 2005; Katsuta et al., 2008), it is suggested that discussing the interionic interaction with the effect of the ion volume is appropriate when comparing the present ions because the structures of the ions are relatively less influenced by a heavy atom substitution compared to the case in which a whole ion is exchanged.

Polarizability is another factor responsible for the intermolecular (or interionic) interaction. The polarizability increases with a longer bond length (and thus a larger molecule), according to the charge response kernel model (Iuchi et al., 2002). Because the increased polarizability could soften the force between the charges, the polarizability effect can reasonably explain the tendency for the shear viscosities of the three ILs to decrease, as well as the volume effect. Indeed, the increased polarizability also provides the stronger interionic interaction because of the larger dispersion and inductive forces. However, the trend of the shear viscosities for the ILs is inconsistent with the effects of the dispersion and inductive forces. With regard to the charge population, the study of the atom charges of the ions indicates that the negative charge magnitude of F for  $[\text{XF}_6]^-$  and the positive charge magnitude of the target element for the cations are larger for a heavier ion. The charge localization in the ions should have a stronger interaction with a counter ion than the ions with the delocalized charge distribution, and the stronger interaction between the cation and anion provides the larger shear viscosity in fluids. Accordingly, the calculation results for the charge magnitude of the anion cannot be used to explain the observed heavy atom substitution effect on the shear viscosity in the ILs. Therefore, the present result of the shear viscosity trend of the three types of ILs can be reasonably explained in the context of the interionic interaction arising from the ionic volume effect.

On the other hand, the trend in the surface tension by the heavy atom substitutions is somewhat complicated in comparison with that in the shear viscosity. As listed in Table 1, the surface tension becomes slightly smaller with the heavier element substitution in the aromatic and nonaromatic “cations” but becomes larger with the heavier element substitution in the “anions”. There is an inverse correlation between surface tension and molar volume in molten salts, including ILs (Jin et al., 2008). The change in surface tension for the ILs by the heavy atom replacement in the cation is well explained by the empirical scheme. However, the feature in the anions is evidently the opposite of the predicted heavy atom substitution effect on the surface tension.

In addition to the shear viscosity, the surface tension in conventional neutral molecular liquids increases with a heavier atom substitution (e.g.,  $\gamma$ (fluorobenzene): 26.66 mN/m <

$\gamma$ (chlorobenzene): 32.99 mN/m <  $\gamma$ (bromobenzene): 35.24 mN/m and  $\gamma$ (diethyl ether): 16.65 mN/m <  $\gamma$ (diethyl sulfide): 24.57 mN/m at 298 K (Lide, 2008)). Therefore, the characteristics of the atom substitutions in the anions of ILs are fairly normal for liquids, but the heavy atom substitutions in the aromatic and nonaromatic cations show an unusual feature. It seems that the mass effect is greater than the volume effect for the surface tension as well as the liquid density.

#### 4. Interionic vibrational band

As shown in Fig. 2, the intermolecular vibrational band in molecular liquids is broad and located in the low frequency region below ca. 150 cm<sup>-1</sup>, in contrast to most of the intramolecular vibrational modes. The same is also true for ILs. Actually, a detailed molecular-level understanding of the intermolecular vibrations in molecular liquids, including ILs, is not simple at all. This is because the molecules or ions in liquids are fluctuating, these molecular or ionic fluctuations give different intermolecular or interionic vibrational modes, and such intermolecular or interionic vibrational modes are often coupled to each other and are fairly anharmonic. In addition, the spectral shape is more complicated than simple Gaussian and Lorentzian line shapes which are usually used to express the line shapes of intramolecular or intraionic vibrational modes. However, this spectrum contains a large quantity of microscopic or molecular-level information. Because heavy atom substitutions in ILs do not have a very great effect on the constituent ionic shape in comparison with a whole ion exchange, a specific comparison between ILs with lighter and heavier atom-substituted ions is possible. The details of such a comparison are given below.

##### 4.1 Cation in aromatic ionic liquids

The first example of an atom substitution study of the interionic vibrational dynamics in ILs is C vs. Si for a side group of an imidazolium cation: [C-MIm]<sup>+</sup> vs. [Si-MIm]<sup>+</sup> (Shirota & Castner, 2005). Fig. 5 shows the low-frequency Kerr spectra and fits for the ILs with [NTf<sub>2</sub>]<sup>-</sup> and [BF<sub>4</sub>]<sup>-</sup>. It should be noted that the contributions of the picosecond orientational relaxations were removed from the full Kerr spectra to focus on the vibrational motions in the ILs.

The low-frequency spectral region from ca. 1 to 150 cm<sup>-1</sup> is usually dominated by the intermolecular vibrational components in most neutral molecular liquids. The same is true for ILs, but the spectrum is somewhat shifted to a higher frequency (Shirota & Castner, 2005). The substantial flexibility of the IL cations and anions often leads to low frequency modes, which are found at the same low-frequency region of the spectrum. Fig. 5 shows how sharper Lorentzian features arising from the cation and anion intraionic vibrational modes are superposed on the broad spectra in the 0 to 150 cm<sup>-1</sup> spectral range. For strongly dipolar liquids such as acetonitrile, the dominant contributions to the intermolecular vibrational dynamics arise from librational and density fluctuation (translational) dynamics, with the former dominating the spectral density (Ryu & Stratt, 2004; Madden & Cox, 1981; Madden, 1983; Geiger & Ladanyi, 1988; Geiger & Ladanyi, 1989). Because these motions have a strong overlap on timescale and are in fact likely coupled for such strongly interacting ions as those in the ILs reported here, it is difficult to distinguish between them.

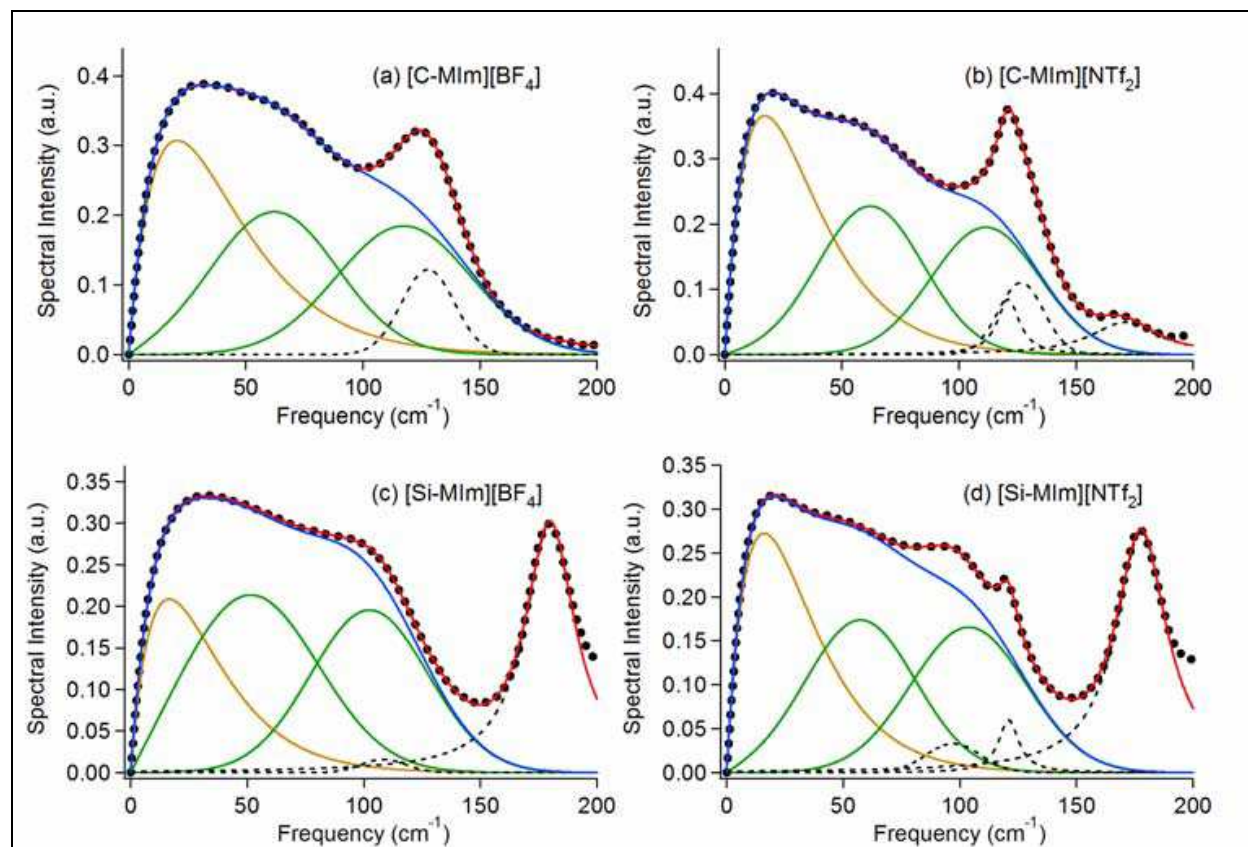


Fig. 5. Low-frequency Kerr spectra of ILs (a) [C-MIm][BF<sub>4</sub>], (b) [C-MIm][NTf<sub>2</sub>], (c) [Si-MIm][BF<sub>4</sub>], and (d) [Si-MIm][NTf<sub>2</sub>]. The black dotted lines, red solid lines, brown solid lines, green solid lines, and black broken lines denote the Fourier-transform Kerr spectra, entire fits, Ohmic components (Eq. 1), antisymmetrized Gaussian components (Eq. 2), and Lorentzian components (intraionic vibrations), respectively. The blue solid lines denote the spectra with the Lorentzian components subtracted.

It is quite likely that the features that fit to Eqs. 1 and 2 cannot be correlated directly with any simple decomposition of the line shape into orientational and translational motions.

From the line-shape features in the interionic vibrational spectra and the line-shape analysis shown in Fig. 5, it becomes clear that (1) the first moments,  $M_1$ , (and the peak frequencies of all model functions) for the [Si-MIm]<sup>+</sup> ILs are lower than those for the [C-MIm]<sup>+</sup> ILs (71.1 cm<sup>-1</sup> for the [C-MIm][BF<sub>4</sub>], 65.8 cm<sup>-1</sup> for the [Si-MIm][BF<sub>4</sub>], 64.3 cm<sup>-1</sup> for the [C-MIm][NTf<sub>2</sub>], and 63.1 cm<sup>-1</sup> for the [Si-MIm][NTf<sub>2</sub>]) and (2) the magnitudes of the differences for the spectral first moments are larger for the [BF<sub>4</sub>]<sup>-</sup> ILs than for the [NTf<sub>2</sub>]<sup>-</sup> ILs.

Considering a harmonic oscillator,  $\omega = (k/\mu)^{1/2}$ , where  $k$  is the force constant and  $\mu$  is the reduced mass, we might expect that the frequencies for such an intermolecular mode would be reduced for the [Si-MIm]<sup>+</sup> ILs relative to the [C-MIm]<sup>+</sup> ILs for at least two reasons: (i) The effective mass for the [Si-MIm]<sup>+</sup> cation is larger than that for the [C-MIm]<sup>+</sup> cation and (ii) the intermolecular interactions for the [Si-MIm]<sup>+</sup> ILs are weaker than those for the [C-MIm]<sup>+</sup> ILs.

In a neutral aprotic molecular liquid, there is a single correlation between the spectral first moment and the square root of the value of surface tension divided by density,  $(\gamma/d)^{1/2}$  (Shirota et al., 2009). The ratios of the surface tensions,  $\gamma([\text{Si-MIm}]^+ \text{ IL})/\gamma([\text{C-MIm}]^+ \text{ IL})$ , are 0.89 for ILs with the  $[\text{BF}_4]^-$  anion and 0.95 for the ILs with the  $[\text{NTf}_2]^-$  anion. Because of the reduction in  $M_1$  by the heavy atom substitution in the cation, the trends are the same, since the difference in liquid density is tiny. We also recall that the ratios of the shear viscosities  $\eta([\text{Si-MIm}]^+ \text{ IL})/\eta([\text{C-MIm}]^+ \text{ IL})$  are 0.135 for ILs with the  $[\text{BF}_4]^-$  anion and 0.625 for the ILs with the  $[\text{NTf}_2]^-$  anion. The interionic vibrational spectrum can be seen to be lower in frequency for the  $[\text{Si-MIm}]^+$  ILs than for the corresponding  $[\text{C-MIm}]^+$  ILs by the first spectral moment. The magnitude of the difference in frequencies resulting from the silicon substitution on the cation does not correlate with the difference in effective mass for either the  $[\text{NTf}_2]^-$  or  $[\text{BF}_4]^-$  ILs. Therefore, the difference in effective mass or liquid density between silicon-substituted and normal IL cations is not the only factor in determining the interionic vibrational frequencies in these four ILs. We think that liquids with lower shear viscosities and surface tensions should have weaker interionic interactions, and thus overall lower frequency interionic vibrational modes, relative to the liquids having higher shear viscosities and surface tensions.

#### 4.2 Anion in aromatic ionic liquids

Next, we compare 1-butyl-3-methylimidazolium  $[\text{BMIm}]^+$  based ILs with a series of hexafluoropnictogenate anions ( $[\text{XF}_6]^-$ : X is P, As, or Sb) (Shirota et al., 2009). As discussed above, the substitution of C by Si in the cation shifts the first moment of the low-frequency spectrum of an IL to a lower value. However, a change in the dipole moment of an ion caused by atom substitution gives a difference in the spectra. Because the hexafluoropnictogenate anion is octahedral, the substitution of a center atom affects the mass and volume (mean polarizability) of the ion, but does not affect the shape (dipole moment and polarizability anisotropy). Thus, it is more ideal to simply examine the atom substitution effects caused by the mass and volume on the interionic vibration in the ILs.

Fig. 6 focuses on the low-frequency Kerr spectra in the frequency range of 0–200  $\text{cm}^{-1}$ . To clearly see the heavy atom substitution effect, the spectral intensities were normalized to make them uniform. To find the regional frequency differences of the low-frequency Kerr spectra for the three ILs, the fit components (Eqs. 1 and 2) are also compared. As shown in the figure, the spectral differences between the three ILs are not very large. However, if we look closely at the low frequency Kerr spectra of the  $[\text{XF}_6]^-$  ILs, there are two meaningful differences. In the higher-frequency region (100–150  $\text{cm}^{-1}$ ), a small spectral difference can be observed: the spectral band shifts to a higher frequency or becomes broader with the smaller  $[\text{XF}_6]^-$  anion of the IL. A clearer heavy atom substitution effect on the interionic vibrational spectrum is seen in the lower frequency region ( $<50 \text{ cm}^{-1}$ ). In addition, the order of the first spectrum moments for the three ILs is  $[\text{BMIm}][\text{PF}_6] > [\text{BMIm}][\text{AsF}_6] > [\text{BMIm}][\text{SbF}_6]$  (69.6  $\text{cm}^{-1}$  for  $[\text{BMIm}][\text{PF}_6]$ , 69.3  $\text{cm}^{-1}$  for  $[\text{BMIm}][\text{AsF}_6]$ , and 68.2  $\text{cm}^{-1}$  for  $[\text{BMIm}][\text{SbF}_6]$ ). The effect of the heavy atom substitution on the interionic vibration (first moment) is similar to the tendency for the shear viscosity, rather than that for the surface tension. However, it is obvious that the tendency for the first spectrum moment in the three ILs is the same as that for the square root of the value of the surface tension divided by the liquid density, which is derived from a simple consideration of a harmonic oscillator, as well as the case for the  $[\text{X-}$

MIm]<sup>+</sup> ILs. That is, the mass effect is significant compared to the interionic interaction effect coming from the ionic volume for the [XF<sub>6</sub>]<sup>-</sup> ILs.

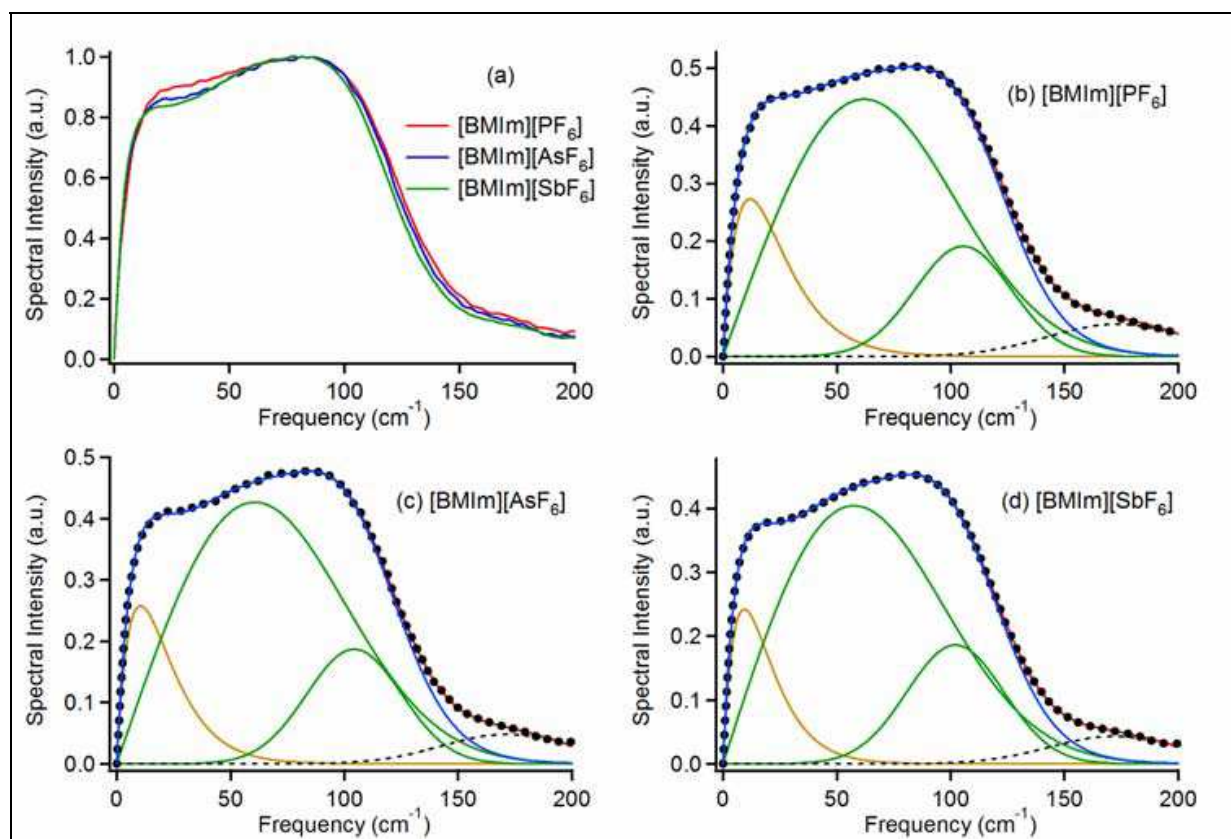


Fig. 6. (a) Normalized low-frequency Kerr spectra of [BMIm][PF<sub>6</sub>] (red), [BMIm][AsF<sub>6</sub>] (blue), and [BMIm][SbF<sub>6</sub>] (green). Low-frequency Kerr spectra and fits for (b) [BMIm][PF<sub>6</sub>], (c) [BMIm][AsF<sub>6</sub>], and (d) [BMIm][SbF<sub>6</sub>]. The black dotted lines, red solid lines, brown solid lines, green solid lines, and black broken lines denote the Fourier-transform Kerr spectra, entire fits, Ohmic components (Eq. 1), antisymmetrized Gaussian components (Eq. 2), and Lorentzian components (intraionic vibrations), respectively. The blue solid lines denote the spectra with the Lorentzian components subtracted.

For further insights, we compare the experimental result with the MD simulation result (Ishida et al., 2009). The decomposition analysis of the computed Kerr spectra based on the MD simulations of the three ILs shows that the composition of the spectrum for the [BMIm][PF<sub>6</sub>] is dominated by the cation-anion cross correlation, while the dominant contribution for the other two ILs is the cation's motion. This indicates that the interionic interaction between the cation and anion becomes weaker with an increase in the volume of the anion, which is in good agreement with the experimental results. The MD simulation work further reveals that the contribution of the reorientation of the cations and anions mainly dominates the Kerr spectrum profile in the three ILs, but the collision-induced and cross (coupling motion) terms do not show large contributions to the Kerr spectrum profile. A comparison between the heavy atom substitution effects of the [XF<sub>6</sub>]<sup>-</sup> anion and [X-MIm]<sup>+</sup> cation on the low-frequency Kerr spectrum provides further detailed aspects for the heavy atom substitution effect on the interionic vibrational dynamics in the aromatic ILs. Let us

recall the key points for the silicon substitution effect of an imidazolium cation ( $[\text{C-MIm}]^+ \rightarrow [\text{Si-MIm}]^+$ ) on the interionic vibrational dynamics discussed above. First, the characteristic frequency such as the first moment of the low-frequency broad spectrum shifts to a lower value with the silicon substitution of the side group from the neopentyl group ( $(\text{CH}_3)_3\text{CCH}_2-$ ) to the trimethylsilylmethyl group ( $(\text{CH}_3)_3\text{SiCH}_2-$ ) of the imidazolium cation. Second, the silicon substitution effect is larger for the  $[\text{BF}_4]^-$  IL than for the  $[\text{NTf}_2]^-$  IL, because the  $[\text{BF}_4]^-$  IL has a larger shear viscosity and surface tension. Third, the silicon substitution effect on the Kerr spectra is clear in the higher frequency region ( $100\text{--}150\text{ cm}^{-1}$ ) than in the lower frequency region ( $<50\text{ cm}^{-1}$ ). From a comparison of the present results for the  $[\text{XF}_6]^-$  ILs with the results for the silicon substitution effect, we find a remarkable point, besides the lower frequency shift in the vibrational band by the heavy atom substitution. The frequency region of the spectral difference caused by the heavy atom substitution for the  $[\text{XF}_6]^-$  ILs is clearly different from that for the  $[\text{X-MIm}]^+$  ILs. It is a lower frequency region for the  $[\text{XF}_6]^-$  ILs and a higher frequency region for the  $[\text{X-MIm}]^+$  ILs.

In the case of aromatic molecular liquids, the intermolecular vibrational dynamics in the lower frequency region, which is typically less than  $50\text{ cm}^{-1}$ , includes the interaction-induced motion, which is translation-like, coupled with the librational motion, which is rotation-like, whereas that in the higher frequency region is predominantly due to the librational motion (Ryu & Stratt, 2004; Elola & Ladanyi, 2006). If the molecular motions and timescale of the interionic vibrational dynamics in the ILs are similar to those of simple aromatic molecular liquids, it would be permissible to consider the origins of the heavy atom substitution effects on the interionic vibrational dynamics in the ILs by taking into account the analogy of simple aromatic liquid dynamics.

The spectral difference for the  $[\text{XF}_6]^-$  ILs is evident in the lower frequency region, and that for the  $[\text{X-MIm}]^+$  ILs is dominant in the higher frequency region. Thus, the interaction-induced (translation-like) motion is sensitive to the heavy atom substitution effect of the  $[\text{XF}_6]^-$  anion, and the substitution for the  $[\text{X-MIm}]^+$  cation is critical for the librational (rotation-like) motion. Why do the heavy atom substitution effects of the  $[\text{X-MIm}]^+$  cation and the  $[\text{XF}_6]^-$  anion on the interionic vibrational spectra appear in the different frequency regions?

It is worthwhile to think of the shapes of the constituent ions of the ILs. Because the  $[\text{XF}_6]^-$  anion has an octahedral symmetry, the effective dipole, which is defined as the vector from the center of mass to the center of charge by Kobrak and co-workers (they called it the "charge arm") (Kobrak & Sandalow, 2006; Li et al., 2008), never changes with the heavy atom substitution of the  $[\text{XF}_6]^-$ . On the other hand, the (static) effective dipole of the  $[\text{X-MIm}]^+$  varies with the heavy atom substitution: the effective dipole of the  $[\text{Si-MIm}]^+$  is approximately 20% larger than that of the  $[\text{C-MIm}]^+$  (Shirota & Castner, 2005).

The nonzero effective dipole of the ion (and the molecule) contributes to both orientational and translational motions, but the zero effective dipole of the ion (and the molecule) never contributes to rotational motion. Accordingly, a comparison between the present and previous studies indicates that the change in the effective dipole (or asymmetric molecular shape) by the heavy atom substitution of the ion provides the dominant heavy atom substitution effect on higher-frequency interionic vibrational dynamics. On the other hand, the change in the pure mass and spherical volume by the heavy atom substitution of the ion gives the large substitution effect on the lower-frequency interionic vibrational dynamics.

Qualitatively, the MD simulation showed the same picture as the experiment (Ishida et al., 2009). The larger masses of As and Sb, compared to P, in the  $[\text{XF}_6]^-$  anion inactivate the translational motion (and its coupling motion with librational motion).

### 4.3 Nonaromatic ionic liquids

Now, let us move to nonaromatic ILs. The unique characteristics of nonaromatic ILs include their flexibility and charge distribution. The comparisons are the ammonium and phosphonium cations, as well as the  $[\text{PF}_6]^-$  and  $[\text{AsF}_6]^-$  anions (Shirota et al., 2010). Fig. 7 shows the low-frequency Kerr spectra of  $[\text{N}_{2228}][\text{NTf}_2]$ ,  $[\text{P}_{2228}][\text{NTf}_2]$ ,  $[\text{N}_{222(2\text{O}_2\text{O}_2)}][\text{NTf}_2]$ , and  $[\text{P}_{222(2\text{O}_2\text{O}_2)}][\text{NTf}_2]$ , and Fig. 8 compares the low-frequency Kerr spectra of  $[\text{N}_{222(2\text{O}_2\text{O}_2)}][\text{PF}_6]$ ,  $[\text{P}_{222(2\text{O}_2\text{O}_2)}][\text{PF}_6]$ ,  $[\text{N}_{222(2\text{O}_2\text{O}_2)}][\text{AsF}_6]$ , and  $[\text{P}_{222(2\text{O}_2\text{O}_2)}][\text{AsF}_6]$ . The results of the line-shape analysis are also shown in the figures. It is clear from these figures that the intensity in the high frequency region ( $>50\text{ cm}^{-1}$ ) is low for the nonaromatic ILs, in comparison with the aromatic ILs (Figs. 5 and 6). A similar feature was also confirmed in conventional molecular liquids (Shirota et al., 2009). Some MD simulations have indicated that the rotation-like motions, such as libration, of aromatic molecules are dominant in the high frequency region, as mentioned before (Ryu & Stratt, 2004; Elola & Ladanyi, 2006). Thus, it seems that the spectral difference in the high frequency region between the aromatic and nonaromatic ILs is caused by the presence or absence of a flat aromatic ring.

The first moments of the low-frequency spectra for the phosphonium-based ILs are slightly lower overall or are similar to those for the ammonium-based ILs, and that the first moment in ILs with the  $[\text{XF}_6]^-$  anion becomes lower through the heavy atom substitution of As for P in the  $[\text{XF}_6]^-$  anion ( $50.6\text{ cm}^{-1}$  for  $[\text{N}_{2228}][\text{NTf}_2]$ ,  $50.0\text{ cm}^{-1}$  for  $[\text{P}_{2228}][\text{NTf}_2]$ ,  $52.3\text{ cm}^{-1}$  for  $[\text{N}_{222(2\text{O}_2\text{O}_2)}][\text{NTf}_2]$ ,  $52.3\text{ cm}^{-1}$  for  $[\text{P}_{222(2\text{O}_2\text{O}_2)}][\text{NTf}_2]$ ,  $66.6\text{ cm}^{-1}$  for  $[\text{N}_{222(2\text{O}_2\text{O}_2)}][\text{PF}_6]$ ,  $64.0\text{ cm}^{-1}$  for  $[\text{P}_{222(2\text{O}_2\text{O}_2)}][\text{PF}_6]$ ,  $64.5\text{ cm}^{-1}$  for  $[\text{N}_{222(2\text{O}_2\text{O}_2)}][\text{AsF}_6]$ , and  $63.5\text{ cm}^{-1}$  for  $[\text{P}_{222(2\text{O}_2\text{O}_2)}][\text{AsF}_6]$ ). A similar feature was observed in aromatic ILs, as seen above (Shirota & Castner, 2005; Shirota et al., 2009). Thus far, we have discussed the change in the interionic vibrational spectra of the ILs caused by the heavy atom substitution in terms of the microscopic interionic interaction. The interionic vibrational frequency decreases with heavy atom substitution. If we consider a harmonic oscillator as a simple model for an interionic vibration, it is clear that the vibrational frequency becomes lower with the weaker interionic interaction because of the heavy atom substitution. The experimental results and ab initio quantum chemistry calculations have shown the nearly neutral charges of the central heteroatoms of the ammonium and phosphonium cations, the large difference in the N-C and P-C bond lengths, and the larger volume of the ion pair for the heavy-atom-substituted ILs. Therefore, it is plausible that the interionic interactions become weaker because of the larger ionic volumes.

On the other hand, the reduced mass is another parameter for the peak frequency of the harmonic oscillator model. The liquid density is substantially increased by the heavy atom substitution of As for P in  $[\text{XF}_6]^-$ , but becomes slightly lower by the substitution of P for N in a cation (Table 1). By an analogy of the better correlation between the first moment of the intermolecular vibrational spectrum and the square root of the value of surface tension divided by liquid density than by formula weight in aprotic molecular liquids (Shirota et al., 2009), we find that the relatively large substitution effect on the low-frequency spectrum in the  $[\text{XF}_6]^-$  ILs could be attributed to the difference in liquid density.

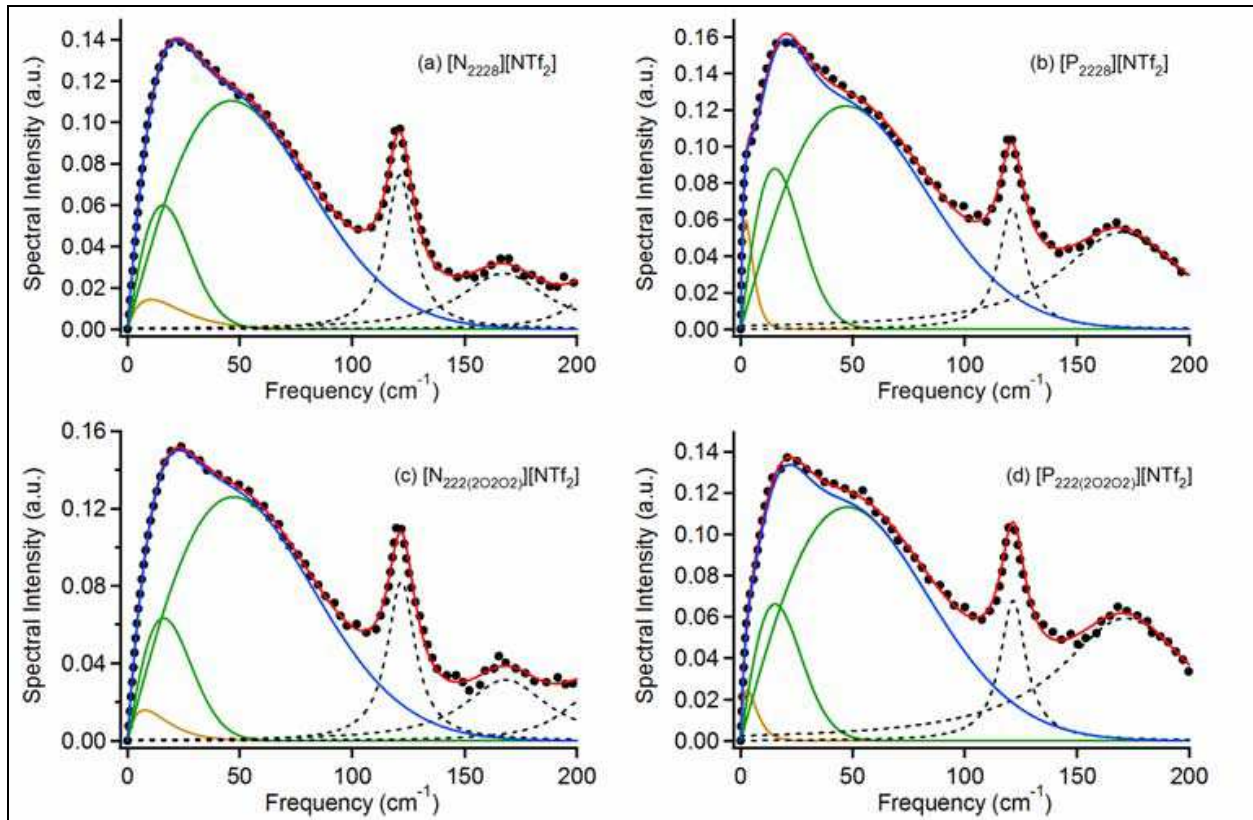


Fig. 7. Low-frequency Kerr spectra and fits for (a)  $[N_{2228}][NTf_2]$ , (b)  $[P_{2228}][NTf_2]$ , (c)  $[N_{222(2O_2O_2)}][NTf_2]$ , and (d)  $[P_{222(2O_2O_2)}][NTf_2]$ . The black dotted lines, red solid lines, brown solid lines, green solid lines, and black broken lines denote the Fourier-transform Kerr spectra, entire fits, Ohmic components (Eq. 1), antisymmetrized Gaussian components (Eq. 2), and Lorentzian components (intraionic vibrations), respectively. The blue solid lines denote the spectra with the Lorentzian components subtracted.

We will further discuss this correlation in the eight ILs later. In any event, the liquid density affects the interionic vibrational spectrum in ILs, as well as the interionic interaction.

We also found that the dual heavy atom substitution effect on the interionic vibrational spectrum of both the cation and anion ( $[N_{222(2O_2O_2)}][PF_6] \rightarrow [P_{222(2O_2O_2)}][AsF_6]$ ) is almost the sum of the respective effects of the cation and anion. In summary, the heavy atom substitution effects on the interionic vibration are rather general for any ion constituents: cation, anion, aromatic, or nonaromatic species.

In addition to the heavy atom substitution effects, we found clear changes caused by the (2-ethoxyethoxy)ethyl group substitution for the octyl group in the cations. The first moment of the low-frequency Kerr spectrum becomes higher with the ether group substitution in both the ammonium and phosphonium cations. The shear viscosity of  $[N_{222(2O_2O_2)}][NTf_2]$  is lower than that of  $[N_{2228}][NTf_2]$  (Table 1). As well as the ammonium-based ILs, phosphonium-based ILs show a similar substitution effect on the shear viscosity. However, the surface tension becomes larger with the substitution of the (2-ethoxyethoxy)ethyl group for the octyl group in the cations. That is, the substitution effect of the ether group

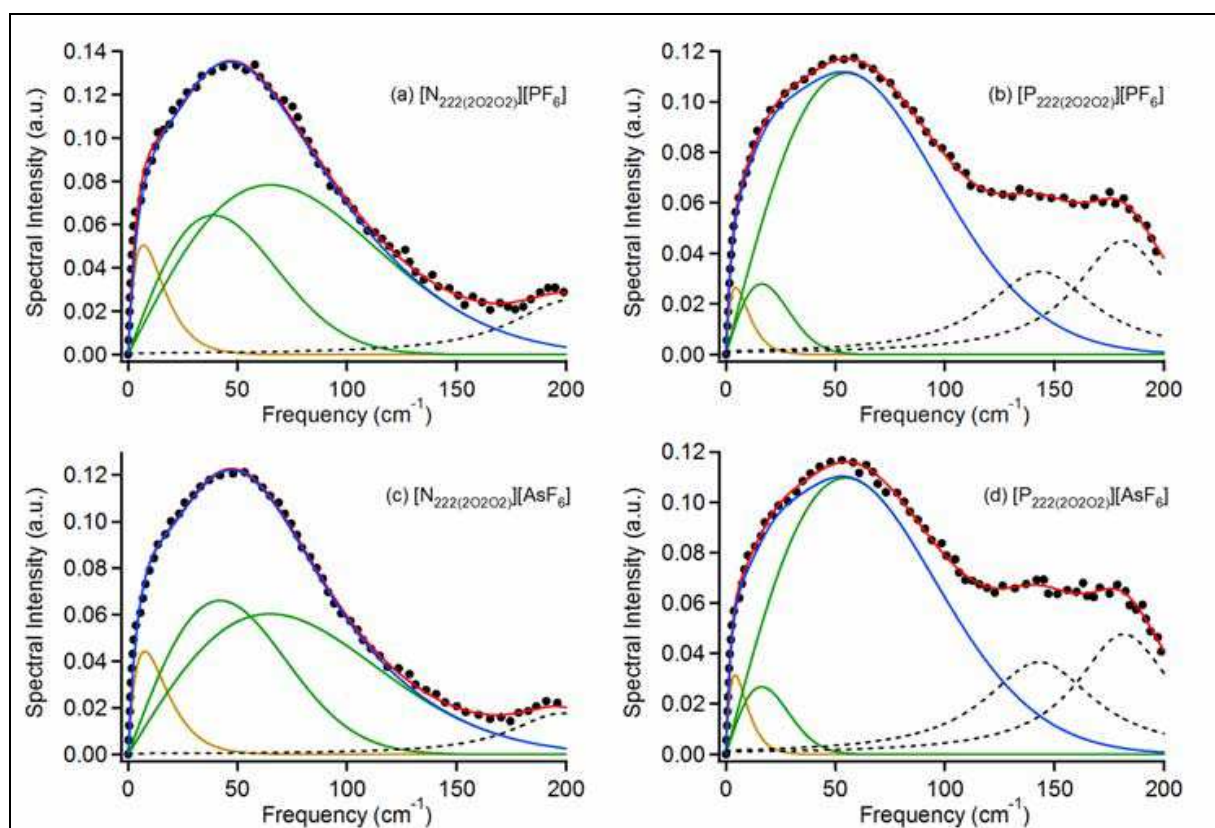


Fig. 8. Low-frequency Kerr spectra and fits for (a)  $[N_{222(20202)}][PF_6]$ , (b)  $[P_{222(20202)}][PF_6]$ , (c)  $[N_{222(20202)}][AsF_6]$ , and (d)  $[P_{222(20202)}][PF_6]$ . The black dotted lines, red solid lines, brown solid lines, green solid lines, and black broken lines denote the Fourier-transform Kerr spectra, entire fits, Ohmic components (Eq. 2), antisymmetrized Gaussian components (Eq. 2), and Lorentzian components (intraionic vibrations), respectively. The blue solid lines denote the spectra with the Lorentzian components subtracted.

on the first moment of the low-frequency Kerr spectrum is similar to that on the surface tension, but not the shear viscosity.

Finally, it might be worth mentioning a comparison between the low-frequency spectrum (microscopic aspect) and bulk property (macroscopic feature) for a broad range of ILs. Unlike conventional molecular liquids (Shirota et al., 2009), the correlations for the ILs are not great. In particular, the correlations of the aromatic and nonaromatic ILs seem to be different (Fujisawa et al., 2009; Shirota et al., 2010). Obviously, ILs are much more complicated than conventional molecular liquids. Because ILs are mixtures of cations and anions in nature and most ILs, particularly ILs containing an ion with a long alkyl group, consist of ionic and hydrophobic parts, the inhomogeneity could give bulk and microscopic interionic/intermolecular interactions that are different from those of neat liquids. Traces of inhomogeneity in ILs were reported in experiments (Triolo et al., 2007; Xiao et al., 2009; Shigeto & Hamaguchi, 2006), as well as MD simulations (Lopes et al., 2006; Wang & Voth, 2006). These natures of ILs surely provide more complicated microscopic features. However, the heavy atom substitution effect on the interionic vibrational band in the ILs is reasonably accounted for by the harmonic oscillator scheme.

## 5. Conclusions

In this chapter, we provided an overview of the heavy atom substitution effects of the constituent ions in some ILs on the static properties such as liquid density, shear viscosity, and surface tension, along with the effects on the interionic vibrational dynamics. With respect to the static properties, we can summarize the heavy atom substitution effects in the ILs as follows.

- The liquid density slightly decreases because of the heavy element substitution from the period 2 element to the period 3 element, but the substitution from the period 3 element to the period 4 element and the period 4 element to the period 5 element substantially increases the liquid density. This complicated feature arises from the counter parameters: volume and mass.
- The shear viscosity is reduced by the heavy atom substitution in any cationic, anionic, aromatic, or nonaromatic species. In addition, the reduction in shear viscosity by a dual cation and anion substitution is simply the sum of the respective effects of the cation and anion substitutions (no synergistic or compensative effect).
- The heavy atom substitution effect on the surface tension shows the same trend as that on the liquid density.

With regard to the interionic vibrational spectrum, the heavy atom substitutions provide a lower frequency shift of the characteristic frequency, the first spectrum moment,  $M_1$ . This feature is observed for both the cation and anion. Comparing the interionic vibrational spectra with the bulk properties, the heavy atom substitution effect on the interionic vibration in the ILs is the same as that on the shear viscosity. The shifts in the interionic vibrational band by heavy atom substitution in both the aromatic and nonaromatic cations are also reasonably accounted for by the feature of the surface tension. However, the substitution in an anion cannot be simply explained by the surface tension. Considering a harmonic oscillator as a simple model, the heavy atom substitution effect on the interionic vibration in the ILs arises from the differences in both the interionic interactions (or volumes) and masses (or liquid densities). The spectral shift in the interionic vibrational band by the heavy atom substitution in the cations is mainly caused by the interionic interaction, whereas the mass effect is large for the substitution in the anions. Although, within the same group, the heavy atom substitution effects on the interionic vibration in the ILs are reasonably taken into account by the harmonic oscillator scheme, the whole picture of the interionic vibrations in ILs still remains unclear. Additional and broader studies will provide a further understanding of the general and deeper aspects of ILs.

## 6. Acknowledgements

We would like to greatly thank the co-workers, Prof. Edward W. Castner, Jr. (Rutgers University), Dr. Tomotsumi Fujisawa (Chiba University), Prof. Tateki Ishida (Institute for Molecular Science), Prof. Keiko Nishikawa (Chiba University), Mr. Kazuya Sugimoto (Chiba University), and Dr. James F. Wishart (Brookhaven National Laboratory). These works were financially supported by the Ministry of Education, Culture, Sports, Science and Technology (MEXT) of Japan (Grant-in-Aids for Special Purposes/Scientific Research (C): 19559001 and Young Scientists (A): 21685001), the Izumi Science and Technology Foundation, and the Futaba Electronics Memorial Foundation.

## 7. References

- Asaki, M. L. T.; Redondo, A.; Zawodzinski, T. A. & Taylor, A. J. (2002). Dielectric relaxation and underlying dynamics of acetonitrile and 1-ethyl-3-methylimidazolium triflate mixtures using THz transmission spectroscopy, *Journal of Chemical Physics*, 116, 10377-10385
- Bondi, A. (1964). van der Waals volumes and radii, *Journal of Physical Chemistry*, 68, 441-451
- Bucaro, J. A. & Litovitz, T. A. (1971). Rayleigh scattering: collisional motions in liquids, *Journal of Chemical Physics*, 54, 3846-3853
- Buffeteau, T.; Grondin, J.; Danten, Y. & Lassegues, J.-C. (2010). Imidazolium-based ionic liquids: quantitative aspects in the far-infrared region, *Journal of Physical Chemistry B*, 114, 7587-7579
- Cang, H.; Li, J. & Fayer, M. D. (2003). Orientational dynamics of the ionic organic liquid 1-ethyl-3-methylimidazolium nitrate, *Journal of Chemical Physics*, 119, 13017-13023
- Castner, E. W., Jr. & Maroncelli, M. (1998). Solvent dynamics derived from optical Kerr effect, dielectric dispersion, and time-resolved Stokes shift measurements: an empirical comparison, *Journal of Molecular Liquids*, 77, 1-36
- Castner, E. W., Jr.; Wishart, J. F. & Shirota, H. (2007). Intermolecular dynamics, interactions, and solvation in ionic liquids, *Accounts of Chemical Research*, 40, 1217-1227
- Chang, Y. J. & Castner, E. W., Jr. (1993). Fast responses from "slowly relaxing" liquids: a comparative study of the femtosecond dynamics of triacetin, ethylene glycol, and water, *Journal of Chemical Physics*, 99, 7289-7299
- Dominguez-Vidal, A.; Kaun, N.; Ayora-Canada, M. J. & Lendl, B. (2007). Probing intermolecular interactions in water/ionic liquid mixtures by far-infrared spectroscopy, *Journal of Physical Chemistry B*, 111, 4446-4452
- Dzyuba, S. V. & Bartsch, R. A. (2002). Influence of structural variations in 1-alkyl(aralkyl)-3-methylimidazolium hexafluorophosphates and bis(trifluoronethylsulfonyl)imides on physical properties of the ionic liquids, *CHEMPHYSICHEM*, 3, 161-166
- Elola, M. D. & Ladanyi, B. M. (2006). Molecular dynamics study of polarizability anisotropy relaxation in aromatic liquids and its connection with local structure, *Journal of Physical Chemistry B*, 110, 15525-15541
- Farrer, R. A. & Fourkas, J. T. (2003). Orientational dynamics of liquids confined in nanoporous sol-gel glass studied by optical Kerr effect spectroscopy, *Accounts of Chemical Research*, 36, 605-612
- Fujisawa, T.; Nishikawa, K. & Shirota, H. (2009). Comparison of interionic/intermolecular vibrational dynamics between ionic liquids and concentrated electrolyte solutions, *Journal of Chemical Physics*, 131, 244519/1-14
- Fumino, K.; Wulf, A. & Ludwig, R. (2008). The cation-anion interaction in ionic liquids probed by far-infrared spectroscopy, *Angewandte Chemie - International Edition*, 47, 3830-3834
- Geiger, L. C. & Ladanyi, B. M., (1988). Higher-order interaction-induced effects on the allowed Raman spectra of liquid CS<sub>2</sub>, *Journal of Chemical Physics*, 89, 6588-6599
- Geiger, L. C. & Ladanyi, B. M., (1989). Molecular dynamics simulation study of nonlinear optical response of fluids, *Chemical Physics Letters*, 159, 413-420

- Giraud, G.; Gordon, C. M.; Dunkin, I. R. & Wyne, K. (2003). The effects of anion and cation substitution on the ultrafast solvent dynamics of ionic liquids: a time-resolved optical Kerr-effect spectroscopic study, *Journal of Chemical Physics*, 119, 464-477
- Hansen, J.-P. & McDonald, I. R. (2006). *Theory of Simple Liquids*, 3rd ed., Academic Press, ISBN 978-0-12-370535-8, London
- Heisler, I. A. & Meech, S. R. (2010). Low-frequency modes of aqueous alkali halides solutions: glimpsing the hydrogen bonding vibration, *Science*, 327, 857-860
- Holbrey, J. D. & Seddon, K. R. (1999). The phase behaviour of 1-alkyl-3-methylimidazolium tetrafluoroborates; ionic liquids and ionic liquid crystals, *Journal of Chemical Society, Dalton Transaction*, 2133-2139
- Hu, Z.; Huang, X.; Annapureddy, H. V. R. & Margulis, C. J. (2008). Molecular dynamics study of the temperature-dependent optical Kerr effect spectra and intermolecular dynamics of room temperature ionic liquid 1-methoxyethylpyridinium dicyanoamide, *Journal of Physical Chemistry B*, 112, 7837-7849
- Hunt, N. T.; Jaye, A. A. & Meech, S. R. (2007). Ultrafast dynamics in complex fluids observed through the ultrafast optically-heterodyne-detected optical-Kerr-effect (OHD-OKE), *Physical Chemistry Chemical Physics*, 9, 2167-2180
- Hyun, B.-R.; Dzyuba, S. V.; Bartsch, R. A. & Quitevis, E. L. (2002). Intermolecular dynamics of room-temperature ionic liquids: femtosecond optical Kerr effect measurements on 1-alkyl-3-ethylimidazolium bis((trifluoromethyl)sulfonyl)imides, *Journal of Physical Chemistry A*, 106, 7579-7585.
- Ishida, T.; Nishikawa, K. & Shirota, H. (2009). Atom substitution effects of  $[XF_6]^-$  in ionic liquids. 2. Theoretical study, *Journal of Physical Chemistry B*, 113, 9840-9851
- Israelachvili, J. N. (1992). *Intermolecular and Surface Forces*, 2nd Ed., Academic Press, ISBN 0-12-375181-0, London
- Iuchi, S.; Morita, A. & Kato, S. (2002). Molecular dynamics simulation with the charge response kernel: vibrational spectra of liquid water and *N*-methylacetamide in aqueous solution, *Journal of Physical Chemistry B*, 106, 3466-3476
- Iwata, K.; Okajima, H.; Saha, S. & Hamaguchi, H. (2007). Local structure formation in alkyl-imidazolium-based ionic liquids as revealed by linear and nonlinear Raman spectroscopy, *Accounts of Chemical Research*, 40, 1174-1181
- Jin, H.; O'Hare, B.; Dong, J.; Arzhantsev, S.; Baker, G. A.; Wishart, J. F.; Benesi, A. J. & Maroncelli, M. (2008). Physical properties of ionic liquids consisting of the 1-butyl-3-methylimidazolium cation with various anions and the bis(trifluoromethylsulfonyl)imide anion with various cations, *Journal of Physical Chemistry B*, 112, 81-92
- Katsuta, S.; Imai, K.; Kudo, Y.; Takeda, Y.; Seki, H. & Nakakoshi, M. (2008). Ion pair formation of alkylimidazolium ionic liquids in dichloromethane, *Journal of Chemical Engineering Data*, 53, 1528-1532
- Khalil, M.; Golonzka, O.; Demirdoven, N.; Fecko, C. J. & Tokmakoff, A. (2000). Polarization-selective femtosecond Raman spectroscopy of isotropic and anisotropic vibrational dynamics in liquids, *Chemical Physics Letters*, 321, 231-237

- Kinoshita, S.; Kai, Y.; Ariyoshi, T. & Shimada, Y. (1996). Low frequency modes probed by time-domain optical Kerr effect spectroscopy, *International Journal of Modern Physics B*, 10, 1229–1272
- Koeberg, M.; Wu, C.-C.; Kim, D. & Bonn, M. (2007). THz dielectric relaxation of ionic liquid:water mixtures, *Chemical Physics Letters*, 439, 60-64
- Kobrak, M. N. & Sandalow, N. (2006). An electrostatic interaction of structure-property relationships in ionic liquids, In: *Molten Salts XIV*, Mantz, R. A., Ed., 417-425, Electrochemical Society, ISBN 978-156677514-4, Pennington
- Li, H.; Ibrahim, M.; Agberemi, I. & Kobrak, M. N. (2008). The relationship between ionic structure and viscosity in room-temperature ionic liquids, *Journal of Chemical Physics*, 129, 124507/1-12
- Li, J.; Wang, I.; Fruchey, K. & Fayer, M. D. (2006). Dynamics in supercooled ionic organic liquids and mode coupling theory analysis, *Journal of Physical Chemistry A*, 110, 10384-10391
- Lide, D. R., Editor-in-Chief (2008). *CRC Handbook of Chemistry and Physics*, 89th Ed., CRC Press, ISBN 978-1-4200-6679-1, Boca Raton
- Lopes, J. N. C.; Gomes, M. F. C. & Padua, A. A. H. (2006). Nonpolar, polar, and associating solutes in ionic liquids, *Journal of Physical Chemistry B*, 110, 16816-16818
- Lotshaw, W. T.; McMorrow, D.; Thantun, N.; Melinger, J. S. & Kitchenham, R. (1995). Intermolecular vibrational coherence in molecular liquids, *Journal of Raman Spectroscopy*, 26, 571-583
- Madden, P. A. & Cox, T. I. (1981). A comparative study of the interaction-induced spectra of liquid CS<sub>2</sub>. II. Lineshapes. *Molecular Physics*, 43, 287-305
- Madden, P. A. (1984). Interaction-induced phenomena, In: *Molecular Liquids – Dynamics and Interactions*, Barnes, A. J.; Orville-Thomsa, W. J. & Yarwood, J., Eds., 431-451, D. Reidel Publishing Company, ISBN 90-277-1817-2, Dordrecht
- McMorrow, D.; Lotshaw, W. T. & Kenney-Wallace, G. A. (1988). Femtosecond optical Kerr effect studies on the origin of the nonlinear responses in simple liquids, *IEEE Journal of Quantum Electronics*, 24, 443-454
- McMorrow, D. & Lotshaw, W. T. (1990). The frequency response of condensed-phase media to femtosecond optical pulses: spectral-filter effects, *Chemical Physics Letters*, 174, 85-94
- McMorrow, D. & Lotshaw, W. T. (1991). Intermolecular dynamics in acetonitrile probed with femtosecond Fourier transform Raman spectroscopy, *Journal of Physical Chemistry*, 95, 10395-10406
- McQuarrie, D. A. (2000). *Statistical Mechanics*, University Science Books, ISBN 1-891389-15-7, Sausalito
- Mukamel, S. (1995). *Principles of Nonlinear Spectroscopy*, Oxford University Press, ISBN 0-19-509278-3, New York
- Nagata, Y. & Tanimura, Y. (2006). Two-dimensional Raman spectra of atomic solids and liquids, *Journal of Chemical Physics*, 124, 024508/1-9
- Ohno, H., Ed. (2005). *Electrochemical Aspects of Ionic Liquids*, ISBN 978-0-471-64851-2, Wiley-Interscience, Hoboken

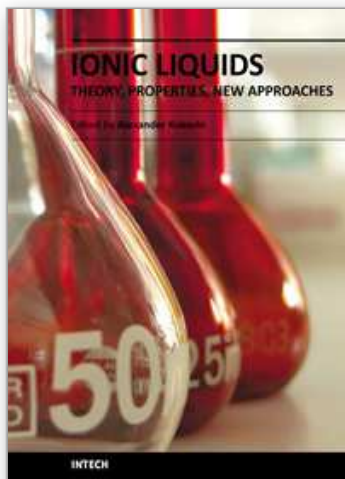
- Rajian, J. R.; Li, S.; Bartsch, R. A.; Quitevis, E. L. (2004). Temperature-dependence of the low-frequency spectrum of 1-pentyl-3-methylimidazolium bis(trifluoromethanesulfonyl)imide studied by optical Kerr effect spectroscopy, *Chemical Physics Letters*, 393, 372-377
- Righini, R. (1993). Ultrafast optical Kerr effect in liquids and solids, *Science*, 262, 1386-1390
- Russina, O.; Triolo, A.; Gontrani, L.; Caminiti, R.; Xiao, D.; Hines, L. G., Jr.; Bartsch, R. A.; Quitevis, E. L.; Plechkova, N. & Seddon, K. R. (2010). Morphology and intermolecular dynamics of 1-alkyl-3-methylimidazolium bis((trifluoromethane)sulfonyl)amide ionic liquids: structural and dynamic evidence of nanoscale segregation, *Journal of Physics: Condensed Matter*, 21, 424121/1-9
- Ryu, S. & Stratt, R. M. (2004). A case study in the molecular interpretation of optical Kerr effect spectra: Instantaneous-normal-mode analysis of the OKE spectrum of liquid benzene, *Journal of Physical Chemistry B*, 108, 6782-6795
- Seki, S.; Hayamizu, K.; Tsuzuki, S.; Fujii, K.; Umebayashi, Y.; Mitsugi, T.; Kobayashi, T.; Ohno, Y.; Kobayashi, Y.; Mita, Y.; Miyashiro, H. & Ishiguro, S. (2009). Relationships between center atom species (N, P) and ionic conductivity, viscosity, density, self-diffusion coefficient of quaternary cation room-temperature ionic liquids, *Physical Chemistry Chemical Physics*, 11, 3509-3514
- Shigeto, S. & Hamaguchi, H. (2006). Evidence for mesoscopic local structures in ionic liquids: CARS signal spatial distribution of  $C_n\text{mim}[\text{PF}_6]$  ( $n = 4,6,8$ ), *Chemical Physics Letters*, 427, 329-332
- Shirota, H. (2005). Ultrafast molecular dynamics of liquid aromatic molecules and the mixtures with  $\text{CCl}_4$ , *Journal of Chemical Physics*, 122, 044514/1-12
- Shirota, H. & Castner, E. W., Jr. (2005). Physical properties and intermolecular dynamics of an ionic liquid compared with its isoelectronic neutral binary solution, *Journal of Physical Chemistry A*, 109, 9388-9392
- Shirota, H. & Castner, E. W., Jr. (2005). Why are viscosities lower for ionic liquids with  $-\text{CH}_2\text{Si}(\text{CH}_3)_3$  vs  $-\text{CH}_2\text{Si}(\text{CH}_3)_2$  substitutions on the imidazolium cations?, *Journal of Physical Chemistry B*, 109, 21576-21585
- Shirota, H.; Funston, A. M.; Wishart, J. F. & Castner, E. W., Jr., (2005). Ultrafast dynamics of pyrrolidinium cation ionic liquids, *Journal of Chemical Physics*, 122, 184512/1-12
- Shirota, H.; Wishart, J. F. & Castner, E. W., Jr. (2007). Intermolecular interactions and dynamics of room temperature ionic liquids that have silyl and siloxy-substituted imidazolium cations, *Journal of Physical Chemistry B*, 111, 4819-4829
- Shirota, H.; Nishikawa, K. & Ishida, T. (2009). Atom substitution effects of  $[\text{XF}_6]^-$  in ionic liquids. 1. Experimental study, *Journal of Physical Chemistry B*, 113, 9831-9839
- Shirota, H.; Fujisawa, T.; Fukazawa, H. & Nishikawa, K. (2009). Ultrafast dynamics in aprotic molecular liquids: a femtosecond Raman-induced Kerr effect spectroscopic study, *Bulletin of the Chemical Society of Japan*, 82, 1347-1366
- Shirota, H.; Fukazawa, H.; Fujisawa, T. & Wishart, J. F. (2010). Heavy atom substitution effects in non-aromatic ionic liquids: Ultrafast dynamics and physical properties, *Journal of Physical Chemistry B*, 114, 9400-9412

- Smith, N. A. & Meech, S. R. (2002). Optically-heterodyne-detected optical Kerr effect (OHD-OKE): applications in condensed phase dynamics, *International Reviews in Physical Chemistry*, 21, 75-100
- Suarez, P. A. Z.; Einloft, S.; Duflus, J. E. L.; de Souza, R. F. & Dupont, J. (1998). Synthesis and physical-chemical properties of ionic liquids based on 1-n-butyl-3-methylimidazolium cation, *Journal de Chimie Physique et de Physico-Chimie Biologique*, 95, 1626-1639
- Tanimura, Y. & Mukamel, S. (1993). Two-dimensional femtosecond vibrational spectroscopy of liquids, *Journal of Chemical Physics*, 99, 9496-9511
- Triolo, A.; Russina, O.; Bleif, H.-J. & Di Cola, E. (2007). Nanoscale segregation in room temperature ionic liquids, *Journal of Physical Chemistry B*, 111, 4641-4644
- Tsunashima, K. & Sugiya, M. (2007). Physical and electrochemical properties of low-viscosity phosphonium ionic liquids as potential electrolytes, *Electrochemistry Communications*, 9, 2353-2358
- Tsuzuki, S.; Tokuda, H.; Hayamizu, K. & Watanabe, M. (2005). Magnitude and directionality of interaction in ion pairs of ionic liquids: relationship with ionic conductivity, *Journal of Physical Chemistry B*, 109, 16474-16481
- Turton, D. A.; Hunger, J.; Stoppa, A.; Hefter, G.; Thoman, A.; Walther, M.; Buchner, R. & Wynne, K. (2009). Dynamics of imidazolium ionic liquids from a combined dielectric relaxation and optical Kerr effects study: evidence for mesoscopic aggregation, *Journal of the American Chemical Society*, 131, 11140-11146
- Urahata, S. M. & Ribeiro, M. C. C. (2005). Single particle dynamics in ionic liquids of 1-alkyl-3-methylimidazolium cations, *Journal of Chemical Physics*, 122, 024511/1-9
- Wang, Y. & Voth, G. A. (2006). Tail aggregation and domain diffusion in ionic liquids, *Journal of Physical Chemistry B*, 110, 18601-18608
- Wasserscheid, P. & Welton, T., Eds. (2008). *Ionic Liquids in Synthesis*, 2nd Ed., WILEY-VCH, ISBN 978-3-527-31239-9, Weinheim
- Wiewior, P. P.; Shirota, H. & Castner, E. W., Jr. (2002). Aqueous dimethyl sulfoxide solutions: Inter- and intra-molecular dynamics, *Journal of Chemical Physics*, 116, 4643-4654
- Xiao, D.; Rajian, J. R.; Hines, L. G., Jr.; Li, S.; Bartsch, R. A. & Quitevis, E. L. (2006). Additivity in the optical Kerr effect spectra of binary ionic liquid mixtures: implications for nanostructural organization, *Journal of Physical Chemistry B*, 110, 16174-16178
- Xiao, D.; Rajian, J. R.; Cady, A.; Li, S.; Bartsch, R. A. & Quitevis, E. L. (2007). Nanostructural organization and anion effects on the temperature dependence of the optical Kerr effect spectra of ionic liquids, *Journal of Physical Chemistry B*, 111, 4669-4677
- Xiao, D.; Rajian, J. R.; Hines, L. G., Jr.; Li, S.; Bartsch, R. A. & Quitevis, E. L. (2008). Nanostructural Organization and anion effects in the optical Kerr effect spectra of binary ionic liquids mixtures, *Journal of Physical Chemistry B*, 112, 13316-13325
- Xiao, D.; Hines, L. G., Jr.; Li, S.; Bartsch, R. A.; Quitevis, E. L.; Russina, O. & Triolo, A. (2009). Effect of cation symmetry and alkyl chain length on the structure and intermolecular dynamics of 1,3-dialkylimidazolium bis(trifluoromethanesulfonyl)amide, *Journal of Physical Chemistry B*, 113, 6426-6433

- Yamamoto, K.; Tani, M. & Hangyo, M. (2007). Terahertz time-domain spectroscopy of imidazolium ionic liquids, *Journal of Physical Chemistry B*, 111, 4854-4859
- Zhong, Q. & Fourkas, J. T. (2008). Optical Kerr effect spectroscopy of simple liquids, *Journal of Physical Chemistry*

IntechOpen

IntechOpen



## **Ionic Liquids: Theory, Properties, New Approaches**

Edited by Prof. Alexander Kokorin

ISBN 978-953-307-349-1

Hard cover, 738 pages

**Publisher** InTech

**Published online** 28, February, 2011

**Published in print edition** February, 2011

Ionic Liquids (ILs) are one of the most interesting and rapidly developing areas of modern physical chemistry, technologies and engineering. This book, consisting of 29 chapters gathered in 4 sections, reviews in detail and compiles information about some important physical-chemical properties of ILs and new practical approaches. This is the first book of a series of forthcoming publications on this field by this publisher. The first volume covers some aspects of synthesis, isolation, production, modification, the analysis methods and modeling to reveal the structures and properties of some room temperature ILs, as well as their new possible applications. The book will be of help to chemists, physicists, biologists, technologists and other experts in a variety of disciplines, both academic and industrial, as well as to students and PhD students. It may help to promote the progress in ILs development also.

### **How to reference**

In order to correctly reference this scholarly work, feel free to copy and paste the following:

Hideaki Shirota and Hiroki Fukazawa (2011). Atom Substitution Effects in Ionic Liquids: A Microscopic View by Femtosecond Raman-Induced Kerr Effect Spectroscopy, *Ionic Liquids: Theory, Properties, New Approaches*, Prof. Alexander Kokorin (Ed.), ISBN: 978-953-307-349-1, InTech, Available from:

<http://www.intechopen.com/books/ionic-liquids-theory-properties-new-approaches/atom-substitution-effects-in-ionic-liquids-a-microscopic-view-by-femtosecond-raman-induced-kerr-effe>

# **INTECH**

open science | open minds

### **InTech Europe**

University Campus STeP Ri  
Slavka Krautzeka 83/A  
51000 Rijeka, Croatia  
Phone: +385 (51) 770 447  
Fax: +385 (51) 686 166  
[www.intechopen.com](http://www.intechopen.com)

### **InTech China**

Unit 405, Office Block, Hotel Equatorial Shanghai  
No.65, Yan An Road (West), Shanghai, 200040, China  
中国上海市延安西路65号上海国际贵都大饭店办公楼405单元  
Phone: +86-21-62489820  
Fax: +86-21-62489821

© 2011 The Author(s). Licensee IntechOpen. This chapter is distributed under the terms of the [Creative Commons Attribution-NonCommercial-ShareAlike-3.0 License](#), which permits use, distribution and reproduction for non-commercial purposes, provided the original is properly cited and derivative works building on this content are distributed under the same license.

IntechOpen

IntechOpen